Polyphosphoinositides Are Enriched in Plant Membrane Rafts and Form Microdomains in the Plasma Membrane[1][W]

Fabienne Furt[2], Sabine König[3], Jean-Jacques Bessoule, Françoise Sargueil, Rémi Zallot, Thomas Stanislas[4], Elodie Noirot, Jeanine Lherminier, Françoise Simon-Plas, Ingo Heilmann, and Sébastien Mongrand*

Laboratoire de Biogenèse Membranaire, UMR 5200, CNRS-Université Victor Segalen Bordeaux 2, 33076 Bordeaux, France (F.F., J.-J.B., F.S., R.Z., T.S., S.M.); Department of Plant Biochemistry, Georg-August-University Göttingen, 37077 Goettingen, Germany (S.K., I.H.); and UMR Plante-Microbe-Environnement 1088, INRA 5184, CNRS-Université de Bourgogne, 21065 Dijon, France (E.N., J.L., F.S.-P.)

In this article, we analyzed the lipid composition of detergent-insoluble membranes (DIMs) purified from tobacco (*Nicotiana tabacum*) plasma membrane (PM), focusing on polyphosphoinositides, lipids known to be involved in various signal transduction events. Polyphosphoinositides were enriched in DIMs compared with whole PM, whereas all structural phospholipids were largely depleted from this fraction. Fatty acid composition analyses suggest that enrichment of polyphosphoinositides in DIMs is accompanied by their association with more saturated fatty acids. Using an immunogold-electron microscopy strategy, we were able to visualize domains of phosphatidylinositol 4,5-bisphosphate in the plane of the PM, with 60% of the epitope found in clusters of approximately 25 nm in diameter and 40% randomly distributed at the surface of the PM. Interestingly, the phosphatidylinositol 4,5-bisphosphate cluster formation was not significantly sensitive to sterol depletion induced by methyl-β-cyclodextrin. Finally, we measured the activities of various enzymes of polyphosphoinositide metabolism in DIMs and PM and showed that these activities are present in the DIM fraction but not enriched. The putative role of plant membrane rafts as signaling membrane domains or membrane-docking platforms is discussed.

Polyphosphoinositides are phosphorylated derivatives of phosphatidylinositol (PtdIns) implicated in many aspects of cell function. They control a surprisingly large number of processes in animal, yeast, and plant cells, including exocytosis, endocytosis, cytoskeletal adhesion, and signal transduction not only as second-messenger precursors but also as signaling molecules on their own by interacting with protein partners, allowing spatially selective regulation at the cytoplasm-membrane interface (for review, see Di Paolo and De Camilli, 2006). Polyphosphoinositides also control the activity of ion transporters and channels during biosynthesis or vesicle trafficking (Liu et al., 2005; Monteiro et al., 2005b). In plants, phosphatidylinositol 4,5-bisphosphate [PtdIns(4,5)P_2] is present in very small quantities (for review, see Stevenson et al., 2000; Meijer and Munnik, 2003) and was visualized in vivo by expressing a fluorescent protein (GFP or yellow fluorescent protein) fused to the pleckstrin homology (PH) domain of the human phospholipase C δ1 (PLCδ1) that specifically binds PtdIns(4,5)P_2. The fused protein yellow fluorescent protein-PHPLCδ1 was present in the cytoplasm but concentrated at the plant plasma membrane (PM) in response to salt stress or upon treatment with the PLC inhibitor U73122 (van Leeuwen et al., 2007). In pollen tubes and root hairs, where spatially focused cell expansion occurs, highly localized PtdIns(4,5)P_2 has been evidenced at the membrane tip (Braun et al., 1999; Kost et al., 1999). PtdIns(4,5)P_2 likely functions as an effector of small G proteins at the apex of cells influencing membrane fusion events (Monteiro et al., 2005a). In guard cells, the level of PtdIns(4,5)P_2 increases at the PM upon illumination (Lee et al., 2007). Combining imaging, patch clamp, and genetic evidence, Lee et al. (2007) further proposed that PtdIns (4,5)P_2 is important for stomatal opening. Stomatal guard cells have also been reported to contain phos-

[1] This work was supported by the French Agence Nationale de la Recherche (contract no. Jeune Chercheur 05–45555 "Plant Rafts" to S.M. and contract no. Jeune Chercheure 05–50611 "Vegeraft" to F.S.-P.) and by the German Research Foundation (Emmy-Noether grant no. He3424–1 to S.K. and I.H.).

[2] Present address: Center for Plant Science Innovation, University of Nebraska-Lincoln, Lincoln, NE 68588.

[3] Present address: European Neuroscience Institute Göttingen, Grisebachstraße 5, 37077 Goettingen, Germany.

[4] Present address: Laboratoire Plantes-Microbe-Environnement, UMR INRA 1088/CNRS 5184/Université de Bourgogne, 17 rue Sully, 21065 Dijon, France.

* Corresponding author; e-mail sebastien.mongrand@biomemb.u-bordeaux2.fr.

The author responsible for distribution of materials integral to the findings presented in this article in accordance with the policy described in the Instructions for Authors (www.plantphysiol.org) is: Sébastien Mongrand (sebastien.mongrand@biomemb.u-bordeaux2.fr).

[W] The online version of this article contains Web-only data.

www.plantphysiol.org/cgi/doi/10.1104/pp.109.149823

phatidylinositol 3-phosphate (PtdIns3*P*) and phosphatidylinositol 4-phosphate (PtdIns4*P*), the products of PtdIns 3-kinase and PtdIns 4-kinase activities, respectively. Jung et al. (2002) demonstrated that PtdIns3*P* and PtdIns4*P* play an important role in the modulation of stomatal closing and that reductions in the levels of functional PtdIns3*P* and PtdIns4*P* enhance stomatal opening. Recently, the hyperosmotic stress response was studied in Arabidopsis (*Arabidopsis thaliana*). Several groups (Pical et al., 1999; DeWald et al., 2001; Konig et al., 2007, 2008b) have shown that plants exhibit a transient increase in polyphosphoinositides after hyperosmotic stress, providing a model for comparing constitutive and stress-inducible polyphosphoinositide pools. Under nonstress conditions, structural phospholipids and PtdIns contained 50 to 70 mol % polyunsaturated fatty acids (PUFA), whereas polyphosphoinositides were more saturated (10–20 mol % PUFA; Konig et al., 2007). Upon hyperosmotic stress, polyphosphoinositides with up to 70 mol % PUFA were formed that differed from constitutive species and coincided with a transient loss in unsaturated PtdIns. These patterns indicate the inducible turnover of an unsaturated PtdIns pool and the presence of distinct polyphosphoinositide pools in plant membranes (Konig et al., 2007).

Since these biological phenomena are likely to occur in distinct regions of the PM, it has been our working hypothesis that in plant cells polyphosphoinositides are localized in various microdomains to participate in different cellular functions. Two decades ago, Metcalf et al. (1986) already suggested that the plant PM contains stable immiscible domains of fluid and gel-like lipids using fluorescent lipid and phospholipid probes incorporated into soybean (*Glycine max*) protoplasts prepared from cultured soybean cells. To this day, it has been generally accepted that lipids and proteins of the PM are not homogeneously distributed within membranes but rather form various domains of localized enrichment. The best-characterized membrane domains are membrane rafts (MRs; Pike, 2006). MRs are liquid-ordered subdomains within eukaryotic membranes that are hypothesized to play important roles in a variety of biological functions by coordinating and compartmentalizing diverse sets of proteins to facilitate signal transduction mechanisms, focal regulation of cytoskeleton, and membrane trafficking (for review, see Rajendran and Simons, 2005; Brown, 2006). Both evidenced in plants and animals, MRs are enriched in sphingolipids and sterols and largely deprived in phospholipids (for review, see Brown and London, 2000; Bhat and Panstruga, 2005). Sterols interact preferentially, although not exclusively, with sphingolipids due to their structure and the saturation of their hydrocarbon chains. Because of the rigid nature of the sterol group, sterols have the ability to pack in between the lipids in rafts, serving as molecular spacers and filling voids between associated sphingolipids (Binder et al., 2003). Acyl chains of MR lipids tend to be more rigid and in a less fluid state (Roche et al., 2008). In agreement, the hydrophobic chains of the phospholipids within the raft are more saturated and tightly packed than those of lipids in the surrounding bilayer (Mongrand et al., 2004). MRs can be isolated from PM by extraction with nonionic detergents such as Triton X-100 (TX100) or Brij-98 at low temperatures. Fluid nonraft domains will solubilize while the MRs remain intact and can be enriched after centrifugation, floating in a Suc density gradient. Floating purified fractions, therefore, are called detergent-insoluble membranes (DIMs) or detergent-resistant membranes and are thought to be the biochemical counterpart of in vivo MRs.

In plants, a few results suggest the role in vivo of dynamic clustering of PM proteins, and they refer to plant-pathogen interaction. A cell biology study reported the pathogen-triggered focal accumulation of components of the plant defense pathway in the PM, a process reminiscent of MRs (Bhat et al., 2005). The proteomic analysis of tobacco (*Nicotiana tabacum*) DIMs led to the identification of 145 proteins, among which a high proportion were linked to signaling in response to biotic stress, cellular trafficking, and cell wall metabolism (Morel et al., 2006). Therefore, these domains are likely to constitute, as in animal cells, signaling membrane platforms concentrating lipids and proteins necessary for the generation of signaling molecules of physiological relevance. This hypothesis was confirmed by a quantitative proteomic study describing the dynamic association of proteins with DIMs upon challenge of tobacco cells with an elicitor of defense reaction (Stanislas et al., 2009). Recently, Raffaele et al. (2009) showed that a group of proteins specific to vascular plants, called remorins (REMs), share the biochemical properties of other MR proteins and are clustered into microdomains of approximately 70 nm in diameter in the PM and plasmodesmata in tobacco, providing a link between biochemistry (DIM purification) and imaging (membrane microdomain observation).

Several investigators have previously suggested that PtdIns(4,5)P_2-rich raft assemblies exist in animal cell membranes to provide powerful organizational principles for tight spatial and temporal control of signaling in motility. Laux et al. (2000) demonstrated that PtdIns(4,5)P_2 formed microdomains in the PM of animal cells, and at least part of these microdomains was colocalized with the myristoylated Ala-rich type C kinase substrate, a protein enriched in MRs, and involved in the regulation of the actin cytoskeleton. The relationship between the spatial organization of PtdIns(4,5)P_2 microdomains and exocytotic machineries has been evidenced in rat. Both PtdIns(4,5)P_2 and syntaxin, a protein essential for exocytosis, exhibited punctate clusters in isolated PM. PtdIns(4,5)P_2 also accumulated at sites of cell surface motility together with a Rho-type GTPase. Therefore, PtdIns(4,5)P_2 may coordinate membrane dynamics and actin organization as well as integrate signaling (Aoyagi et al., 2005). These results provide evidence of compartmentaliza-

tion of PtdIns(4,5)P_2-dependent signaling in cell membranes.

Little is known in plants about whether and how separate pools of polyphosphoinositides come about and how they are regulated. In this article, we have analyzed the lipid composition of DIMs enriched from tobacco PM, with a particular focus on phospholipids involved in signaling events, such as polyphosphoinositides. We showed that polyphosphoinositides were enriched in DIMs, whereas structural phospholipids were largely excluded. We were able to calculate that almost half of the PtdIns*P* and PtdIns(4,5)P_2 were present in MR domains. Fatty acid composition analyses demonstrate that this enrichment is accompanied by the presence of more saturated fatty acids in polyphosphoinositides. Consistently, using an electron microscopy approach with immunogold labeling and a pattern-identifying statistical analysis, we showed that more than half of the PtdIns(4,5)P_2 labeling is clustered into microdomains of approximately 25 nm in diameter in the PM. Finally, we measured the activities of lipid-using enzymes present in DIMs/PM and showed that activities responsible for polyphosphoinositide metabolism are present in the DIM fraction.

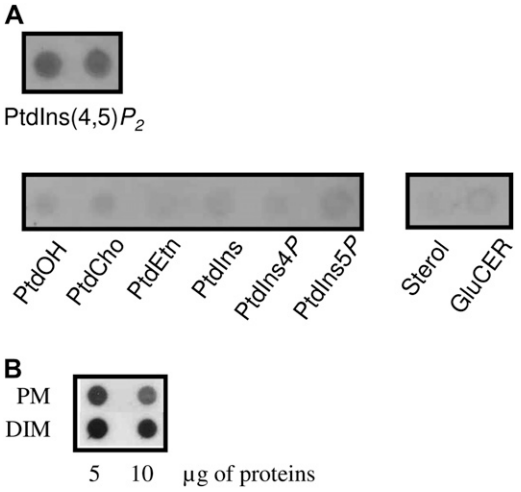

Figure 1. Polyphosphoinositides are enriched in DIMs. A, Specificity of the antibody to PtdIns(4,5)P_2 tested by dot blot and immunodetection. Each lipid solution was dried, and lipids were resuspended in 50 μL of TBS-T, sonicated for 5 min, and plotted on a PVDF membrane. GluCER, Glucosylceramide. B, PtdIns(4,5)P_2 was enriched in DIMs. Five or 10 μg of PM or DIMs purified from BY-2 cells was analyzed by dot blot and immunodetection using an antibody to PtdIns(4,5)P_2.

RESULTS

Are Polyphosphoinositides Enriched in DIMs Purified from Tobacco PM?

To determine whether polyphosphoinositides could be enriched in DIMs, lipids were first spotted onto polyvinylidene difluoride (PVDF) membranes and specific immunodetection was tested using an antibody against PtdIns(4,5)P_2 (Euromedex). In our hands, PtdIns(4,5)P_2 was specifically detected by the antiserum, whereas other lipids were not recognized (Fig. 1A). The specific recognition of other isomers of polyphosphoinositides by the PtdIns(4,5)P_2 monoclonal antibodies was also tested on commercial lipid-blot overlay assays (Supplemental Fig. S5). Based on these results, a nonspecific interaction with anionic phospholipids can be excluded. When tested against all known phosphoinositides, the antibody specifically recognized PtdIns(4,5)P_2, as expected, but also cross-reacted with PtdIns(3,4)P_2 and PtdIns(3,4,5)P_3. As PtdIns(3,5)P_2 or any of the PtdIns monophosphates were not recognized, the antiserum appears to be specific for phosphoinositol head groups that contain two or more adjacent phosphate groups. In light of this characterization, cross-reactivity of the antiserum with PtdIns(3,4)P_2 or PtdIns(3,4,5)P_3 cannot be ruled out in principle. However, taking into account the current knowledge on the occurrence of phosphoinositides in plants, it must be noted that neither endogenous PtdIns(3,4,5)P_3 nor PtdIns(3,4)P_2 has been detected in plants (Heilmann, 2009; Munnik and Testerink, 2009). In contrast, the presence of PtdIns(4,5)P_2 in plant cells has been demonstrated by numerous groups using different methods (DeWald et al., 2001; van Leeuwen et al., 2007; Konig et al., 2008a, 2008b), leading us to conclude that the signals detected are most likely PtdIns(4,5)P_2.

Then, identical amounts of protein from PM and DIM preparations from tobacco BY-2 cell cultures were compared by dot blot using the antibody to PtdIns(4,5)P_2 (Fig. 1B). Signals for PtdIns(4,5)P_2 were clearly detected in both PM and DIM fractions. However, because this technique is not fully quantitative, it is not obvious whether a stronger PtdIns(4,5)P_2 signal in the DIMs reflects a higher abundance of PtdIns(4,5)P_2 in these samples. As immunodetection also gives no indication of the nature of fatty acids associated with the detected lipids, lipids were extracted from PM and DIMs purified from tobacco leaves or BY-2 cells and analyzed as described by Mongrand et al. (2004) and Konig et al. (2008b).

Up to Half of the Polyphosphoinositides Present in Plant PM Is Located in DIM Fractions

Phospholipids, sphingolipids, and sterols were extracted from PM and DIM preparations from tobacco leaves and BY-2 cell cultures by organic solvents and quantified by high-performance thin-layer chromatography (HP-TLC) and subsequent gas chromatography (GC) analyses. Free sterols, sterol conjugates (steryl glucosides + acylated steryl glucosides), and glucosylceramides were largely enriched in DIMs, from 44.3 mol % in leaf PM to 75.3 mol % in DIMs and from 40.5 mol % in BY-2 cell PM to 64.7 mol % in DIMs (Fig. 2). By contrast, major structural glycerolipids, namely

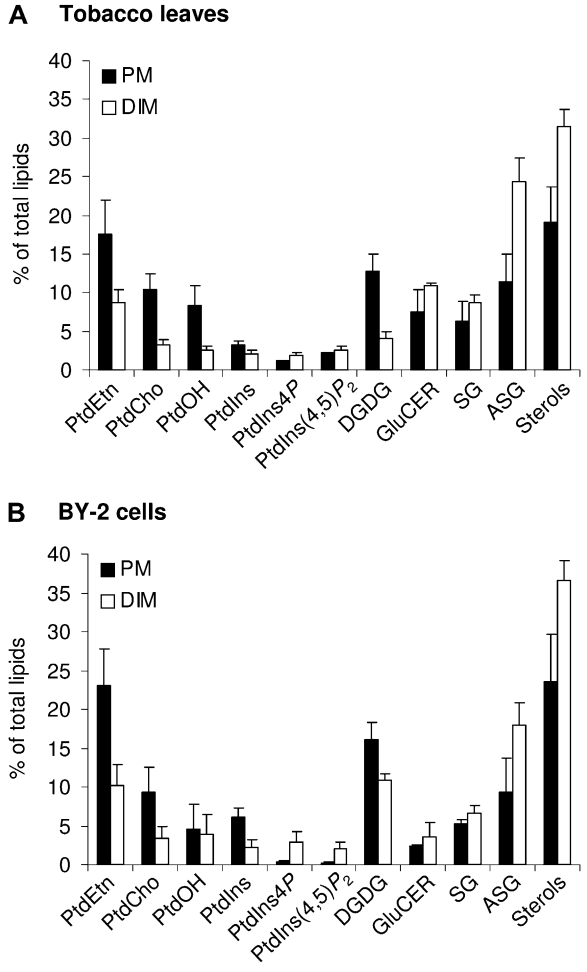

Figure 2. Lipid composition of PM and DIMs from tobacco leaves (A) and BY-2 cells (B). Lipids from membrane fractions were extracted with organic solvent mixture, separated by TLC, and quantified by GC as described in "Materials and Methods." The data are expressed as means of three independent experiments ± SD. SG, Steryl glucoside; ASG, acylated steryl glucoside.

phosphatidylcholine (PtdCho), phosphatidylethanolamine (PtdEtn), phosphatidic acid (PtdOH), digalactosyldiacylglycerol, and PtdIns, were largely excluded from DIMs, with reductions from 52.3 mol % in leaf PM to 20.4 mol % in DIMs and from 59 mol % in BY-2 cell PM to 30.5 mol % in DIMs (Fig. 2). These results are in agreement with previous lipid analyses performed on DIMs purified from *Medicago truncatula* root PM (Lefebvre et al., 2007), from microsomes prepared from Arabidopsis seedlings (Borner et al., 2005), and from tobacco leaf PM and BY-2 cell PM (Mongrand et al., 2004).

Besides major lipids, we focused on polyphosphoinositides using a procedure combining HP-TLC with subsequent GC analysis designed to study such minor lipids (Konig et al., 2008a). Analyses were performed on PM and DIMs purified from tobacco leaves or from BY-2 cells. PtdIns4*P* and PtdIns(4,5)P_2 were found to be the only phospholipids enriched in DIMs when compared with PM preparations from which DIMs originated. In BY-2 cells, the levels of PtdIns4*P* and PtdIns(4,5)P_2 increased from 0.44 mol % in PM to 4.8 mol % in DIMs, corresponding to an 11.0-fold absolute increase (Fig. 2). A minor (1.3-fold) absolute increase of PtdIns4*P* and PtdIns(4,5)P_2 was observed in leaf DIMs.

Considering that DIMs represent only approximately 10% of total PM proteins (Mongrand et al., 2004), we can estimate that 50.0% and 52.7% of the molecules PtdIns4*P* and PtdIns(4,5)P_2, respectively, are present in DIMs of BY-2 cell PM. Similarly, in tobacco leaves, 43.3% and 30.9% of PtdIns4*P* and PtdIns(4,5)P_2 molecules, respectively, segregated in DIMs extracted from PM. Thus, the observed absolute increases indicate a substantial enrichment of polyphosphoinositides in the DIM fractions purified from tobacco leaves and from BY-2 cells.

Polyphosphoinositides Display Highly Saturated Fatty Acids in Both PM and DIMs

We previously described (Mongrand et al., 2004) that the hydrophobic chains of the major structural phospholipids within the tobacco DIMs (namely PtdCho, PtdEtn, phosphatidylserine, PtdIns, and PtdOH) were more saturated than those of structural phospholipids within the whole PM. Here, we show that polyphosphoinositides are the only glycerophospholipids enriched in plant DIM preparations (Figs. 1 and 2). Therefore, to gain insight into the biophysical principles underlying pool formation of polyphosphosinositide molecular species present in DIMs, individual phospholipids, including polyphosphoinositides, were analyzed for their associated fatty acids. As previously shown (Bohn et al., 2001; Konig et al., 2007), structural phospholipids (namely PtdCho, PtdEtn, PtdIns, and PtdOH) in plant PM displayed palmitic acid (16:0) and linoleic acid (18:$2^{\Delta 9,12}$ [x:$y^{\Delta z}$, where x:y is a fatty acid containing x carbons and y double bonds in position z counting from the carboxyl end]) as major fatty acids (Fig. 3). Stearic acid (18:0), oleic acid (18:$1^{\Delta 9}$), and linolenic acid (18:$3^{\Delta 9,12,15}$) can also be detected. In tobacco leaves, the degree of unsaturation of these lipids (given as the number of double bonds per mole of associated lipids) strongly decreased in DIMs compared with PM, from 1.29 to 0.52 in PtdEtn, from 1.31 to 0.46 in PtdCho, from 1.36 to 0.48 in PtdOH, and from 0.74 to 0.40 in PtdIns (Table I). The same pattern was found for BY-2 cells, where the degree of unsaturation decreased from 1.35 to 0.28 in PtdCho, from 1.46 to 0.40 in PtdEtn, from 1.20 to 0.64 in PtdOH, and from 1.21 to 0.41 in PtdIns (Table II).

By contrast, the patterns of fatty acids associated with polyphosphoinositides differed from those found in structural phospholipids (Fig. 3). Indeed, the major fatty acids detected in polyphosphoinositides from PM were 16:0, 18:0, and 18:$1^{\Delta 9}$. Moreover, the degree of unsaturation did not differ between the polyphosphoinositides present in PM preparations and those

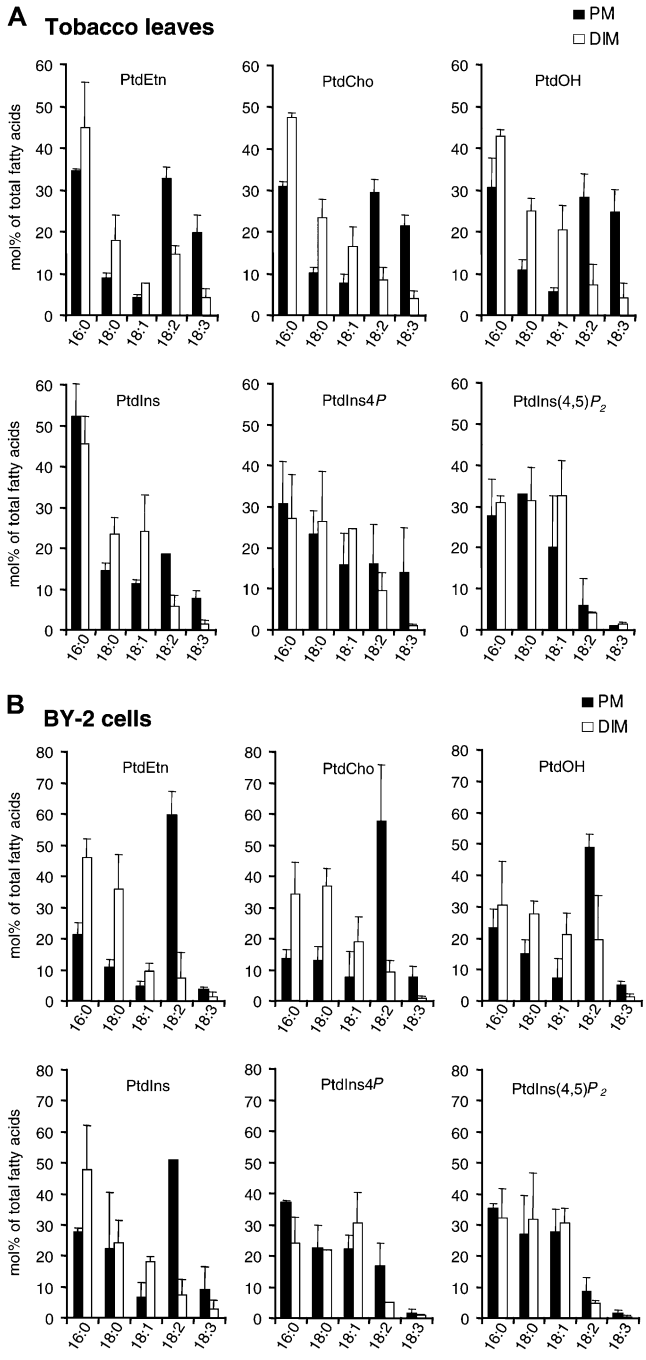

Figure 3. Fatty acid composition of phospholipids from PM and DIMs purified from tobacco leaves and BY-2 cells. Total lipid extracts were subjected to TLC. Individual phospholipids were isolated, and fatty acids were transmethylated and analyzed by GC as described in "Materials and Methods." To compare fatty acid compositions, bars represent mol % of total fatty acids present in each lipid and are means of three independent experiments ± SD.

found in enriched DIMs. In BY-2 cells, the degree of unsaturation of PtdIns4*P* and PtdIns(4,5)P_2 was quite similar, with values around 0.5 in both PM and DIMs (Table II). In tobacco leaves, the calculated value was also around 0.5 for PtdIns(4,5)P_2 originating from either PM or enriched DIMs. The degree of unsaturation for PtdIns4*P* from tobacco leaves decreased from 1.15 in PM to 0.44 in DIMs (Table I). The high level of saturation associated with polyphosphoinositides present in both PM and DIMs is in perfect agreement with the enrichment of these lipids previously observed in DIM fractions (Figs. 1 and 2).

Visualizing PtdIns(4,5)P_2 Enriched in PM Domains of Plant Cells

The results so far indicated that a major proportion of polyphosphoinositides and in particular PtdIns(4,5)P_2 were present in plant MRs. In order to provide additional evidence for this concept, we attempted the visualization of putative PtdIns(4,5)P_2 domains in PM vesicles and analyzed whether PtdIns(4,5)P_2 would partition in a random, a clustered, or a regular pattern in the plane of the PM (Fig. 4A). For these experiments, we modified a method, previously used for the study of the plant raft protein REM (Raffaele et al., 2009), to localize and analyze the distribution of PtdIns(4,5)P_2 on the surface of PM vesicles at a nanometer scale. Briefly, purified BY-2 cell PM vesicles were directly deposited onto microscope grids. The grids were then blocked for nonspecific binding and incubated with primary antibodies and further with secondary IgG conjugated to colloidal gold particles. After fixation with glutaraldehyde, preparations were negatively stained in ammonium molybdate and observed with a transmission electron microscope. The aim was to circumvent technical difficulties previously reported for the "in-batch" immunolocalization: (1) the centrifugation of the gold conjugate could induce gold aggregates in the pellet that stuck to the PM vesicles, producing nonspecific clustering; (2) the difficulties, at the end of the protocol, in spreading the packed vesicles on a microscope grid that did not allow visualization of isolated vesicles; and (3) the use of large quantities of both biological materials and costly antibodies.

The "on-grid" procedure was compared with the previous in-batch procedure using the antibodies to REM, a well-established MR protein in solanaceous plants, which clusters in PM domains of approximately 70 nm diameter (Raffaele et al., 2009). After the deposit of the vesicles onto the grid, we tested different fixative solutions before the in situ immunological assay; however, this step drastically reduced the labeling. Therefore, we resolved to label fresh PM vesicles prior to fixation. In the test method on grid, REM distribution was observed as clusters ranging from 45 to 76 nm at the surface of the vesicles (Fig. 4B), thus reproducing the results presented by Raffaele et al. (2009). The background observed in immunological controls was negligible (Supplemental Fig. S4).

The experiments so far validated the technical feasibility of the applied on-grid protocol. In the next step, we used the specific antibody to PtdIns(4,5)P_2 (Fig. 1A) to study the distribution of this lipid on the

Table I. *Degree of unsaturation of fatty acids in each phospholipid from tobacco leaf PM and DIM*

Sample	PtdEtn	PtdCho	PtdOH	PtdIns	PtdIns4*P*	PtdIns(4,5)P_2
PM	1.29 ± 0.06	1.31 ± 0.03	1.36 ± 0.26	0.74 (n = 2)	1.15 (n = 2)	0.41 (n = 1)
DIM	0.52 (n = 2)	0.46 ± 0.08	0.48 ± 0.15	0.40 ± 0.12	0.44 (n = 2)	0.45 ± 0.10

surface of PM vesicles. The average labeling density was quantified to 180 ± 19 gold particles per μm^2 of vesicle flat surface (n = 3). By computing statistical distances between gold particles, we calculated that 59% ± 4.3% (n = 3) of the gold particles showed a clustered distribution throughout the vesicle surface, with an average diameter of 25 ± 8 nm (Fig. 4C). The distance between these clusters was measured and estimated as 89 ± 38 nm (Fig. 4C). However, 41% of the gold particles exhibited a random distribution on the PM surface, as shown in Figure 4A. These results are in perfect agreement with the biochemical analyses reporting that approximately half of the PtdIns(4,5)P_2 was found associated with DIMs (Fig. 2). Controls including omission of the primary antibody exhibited very weak labeling (Supplemental Fig. S4).

To determine whether PtdIns(4,5)P_2 associated with DIMs is altered by the removal of free sterols after the addition of methyl-β-cyclodextrin (mbCD), we performed immunogold labeling of PtdIns(4,5)P_2 on PM vesicles pretreated with mbCD (biochemical analysis indicated that the free sterol content was reduced by 63%). We previously checked by electron microscopy that treatment with mbCD does not significantly modify the morphology of tobacco PM vesicles but does disorganize the clustering of REM in the plane of the PM bilayer (Raffaele et al., 2009). On the surface of PtdIns(4,5)P_2-labeled vesicles, 57% of the gold particles appeared in a clustered pattern whereas 43% showed a random distribution (Fig. 4D). The average labeling density was recorded as 142 gold particles per μm^2 of PM vesicle surface. The average radius of the clusters was measured as 25 ± 11 nm, and the mean distance between clusters was estimated as 89 ± 38 nm. These results are very similar to those obtained without mbCD treatment and suggest that both distributions of PtdIns(4,5)P_2, random and clustered, could coexist at the scale of a MP vesicle whose surface could be estimated to 0.035 μm^2.

Activities of Signaling Lipid-Modifying Enzymes Are Present in PM and DIMs

The fact that polyphosphoinositides were enriched in the DIM fractions prompted us to assay the enzyme activities that might directly or indirectly be responsible for the synthesis or degradation of relevant lipids in DIMs compared with the PM from which the DIM preparations were derived (Fig. 5). PLC, phospholipase Dα (PLDα), phospholipase Dβ (PLDβ), PtdIns*P* kinase, PtdIns(4,5)P_2 kinase, PtdOH kinase, and diacylglycerol (DAG) kinase activities were analyzed according to "Materials and Methods."

Enzyme activities were first assayed as a function of the PM protein amount used to check the linearity of the response (Supplemental Fig. S1). Enzyme-specific activities were further calculated by analyzing the slope in the initial linear phase of a time-course study consisting of four time points for each PM fraction and for each exogenous substrate (Supplemental Fig. S2). The initial time points showed a linear relationship between time and product formed. A minimum of three time points was used to calculate the reaction rate for each PM fraction (Supplemental Fig. S2).

Enzyme activities present in raft domains can be determined by analyzing the activity detected in a DIM preparation and comparing it with its detergent-soluble membrane (DSM) counterpart. The main caveat of this procedure is the fact that DSM cannot be pulled down and rinsed from contaminating Suc (52%, w/w) and TX100 (1% [w/w] final) at the bottom of the gradient used. Therefore, an inherent complication of this approach is that DIMs and DSMs are compared under two very different conditions, in particular regarding the immediate environment of the enzyme tested (micellar for DSMs versus membrane for DIMs). In order to enable a meaningful comparison, we decided to compare the lipid-using enzyme activities of DIMs with those of the whole PM, thus avoiding the experimental difficulties mentioned above. However, another particular complication of the DIM analysis arises from the fact that the experimental procedures to purify DIMs last 16 h beyond the preparation of the parental PM. Thus, we decided to prepare "control PM" (C-PM) in the absence of treatment with TX100 that was submitted to the discontinuous Suc gradient under the exact same conditions as applied for the purification of DIMs.

First, C-PM preparations were used to assay the activities of the lipid-modifying enzymes described above. Figure 6 shows that most of the enzymes displayed losses between 10% and 50% of their specific activities in C-PM compared with the activities detected in the original PM. PtdIns*P* kinase was not altered and was even slightly activated in BY-2 cell

Table II. *Degree of unsaturation of fatty acids in each phospholipid from BY-2 cell PM and DIM*

Sample	PtdEtn	PtdCho	PtdOH	PtdIns	PtdIns4*P*	PtdIns(4,5)P_2
PM	1.35 ± 0.15	1.46 ± 0.18	1.20 ± 0.07	1.21 (n = 2)	0.60 ± 0.17	0.49 ± 0.19
DIM	0.28 ± 0.12	0.40 ± 0.07	0.64 ± 0.25	0.41 ± 0.18	0.55 (n = 1)	0.41 ± 0.07

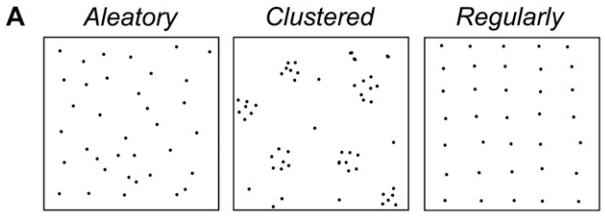

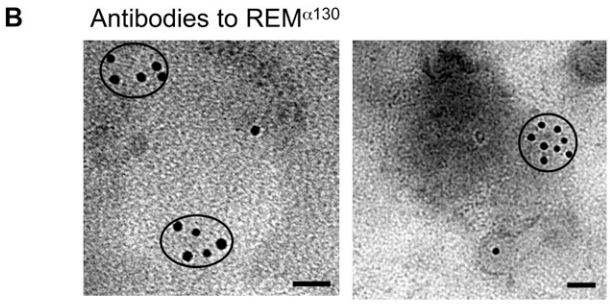

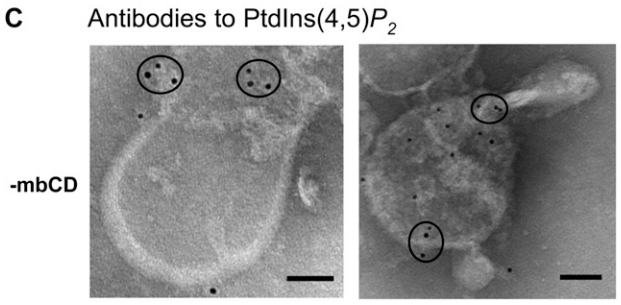

Statistical analysis

	Experiments				
	1	2	3	mean ±SD	Size of clusters
Nb of gold particles	162	180	200	180±19	25nm±8
Percent of gold particles in clusters	63	55	56	58.0%±4.4	

Nb of gold particles	78	67		142	25nm±11
Percent of gold particles in clusters	60	54		57.0%± 4,3	

Figure 4. PtdIns(4,5)P_2 locates in membrane domains in BY-2 cell PM vesicles. A, Theoretical partitioning of gold particles in the plane of the PM. B, Transmission electron micrographs of negatively stained tobacco PM vesicles immunogold labeled on grids with antibodies to REM α130, detected by goat anti-mouse gold complex of 5 nm, and observed by electron microscopy. C and D, Transmission electron micrographs of negatively stained tobacco PM vesicles treated (D) or not (C) with mbCD and immunogold labeled on grids with antibodies to PtdIns(4,5)P_2, detected by goat anti-mouse gold complex of 5 nm, and observed by electron microscopy. Circles indicate obvious membrane domains. Statistical analyses are shown for each condition on the right (−mbCD, $n = 3$; +mbCD, $n = 2$). Bars = 100 nm.

C-PM compared with its corresponding PM preparation. In contrast, DAG kinase activity was very sensitive to the purification procedure, and less than 1% of the activity measured in PM was detected in C-PM from both leaves and BY-2 cell membranes (Fig. 6).

The next step was to compare the activities detected in DIM and C-PM preparations. Specific activities measured in DIMs are expressed as percentages of the specific activities detected in C-PM, both for tobacco leaves and BY-2 cells (Fig. 7). The first surprising observation was that none of the enzymes studied displayed a strict enrichment of their specific activities comparing DIM and C-PM activities. Concerning phospholipases, PLDα or PLDβ activities were detected at low levels in DIMs and represent approximately 10% to 15% of the specific activities found in C-PM preparations. No result for PLDα from leaf DIM was displayed, because of a lack of reproducibility between the biological assays (data not shown). The same is true for PLC, the activity of which varied in DIMs from approximately 35% to 108% of the specific activities assayed in C-PM (data not shown); these results were also not included in Figure 7. As already mentioned, DAG kinase activity was very sensitive to the purifi-

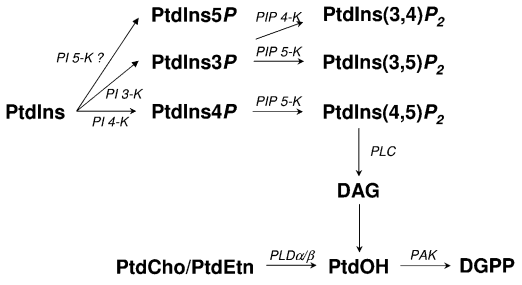

Figure 5. Biosynthetic pathways of signaling phospholipids. Lipid signaling molecules investigated in this study are part of a network of interdependent chemical conversions. DAGK, DAG kinase; InsP_3, inositol trisphosphate; PtdGro, phosphatidylglycerol; PAK, phosphatidic acid kinase; PIK, PtdIns kinase; PI3K, PtdIns 3-kinase; PI4K, PtdIns 4-kinase; PI5K, PtdIns 5-kinase; PIPK, PtdIns phosphate kinase.

cation procedure even in C-PM preparations; consequently, no activity was detected in the corresponding DIM fraction (Fig. 7). PtdOH kinase, which measures the formation of diacylglycerolpyrophosphate (DGPP) from PtdOH, was also assayed, and PtdOH kinase activity detected in DIMs represented up to 20% of that measured in C-PM preparations.

According to the number and the position of the phosphate group, up to six different isoforms of polyphosphoinositides have been reported in plant cells. As a consequence, we needed to discriminate between the different PtdIns 3-, 4-, or 5-kinase and PtdIns*P* 4- or 5-kinase activities (Mueller-Roeber and Pical, 2002). Using an appropriate HP-TLC solvent system, we first determined the nature of PtdIns*P* isomers synthesized from exogenously added PtdIns in tobacco PM (Hegewald, 1996). Only PtdIn4*P* and PtdIns3*P* were synthesized, and no PtdIn5*P* was detected (Supplemental Fig. S3A). Moreover, PtdIns kinase activity assayed in tobacco PM was largely inhibited by wortmannin or adenosine (Supplemental Fig. S3, B and C). Considering also the fact that the major PtdIns kinase in plants is PtdIns 4-kinase (Mueller-Roeber and Pical, 2002), we assumed that the PtdIns kinase detected in PM fractions is a type III PtdIns 4-kinase. In good agreement with this interpretation, type III kinases were previously located in microsomes and particularly in the PM (Mueller-Roeber and Pical, 2002).

Polyphosphoinositide kinase activities, likely reflecting a type III PtdIns 4-kinase and a type I PtdIns4*P* 5-kinase, were detected in the DIM fractions and ranged from approximately 10% to 25% in DIMs prepared from tobacco leaves or from BY-2 cells, respectively, of the values measured in the corresponding C-PM preparations. We also used PtdIns5*P* as exogenously added substrate to assay PtdIns5*P* 4-kinase, but no PtdIns(4,5)P_2 was ever detected on HP-TLC plates, suggesting an absence of type II PtdIns5*P* 4-kinase activity in tobacco PM (n = 10; data not shown). This result is consistent with the absence of the substrate (PtdIn5*P*) in tobacco PM and with a previous genomic screen reporting the lack of a type II PtdIns*P* kinase activity (Mueller-Roeber and Pical, 2002).

DISCUSSION

Polyphosphoinositides Are Enriched in DIMs Originated from Tobacco PM

In addition to their classical roles as second messengers in signal transduction at the cell surface, phosphorylated products of PtdIns play critical roles in the regulation of membrane trafficking as regulators for the recruitment or the activation of proteins essential for cytoskeletal dynamics or vesicular transport. Indeed, local changes in the concentration of polyphosphoinositides, and in particular of PtdIns(4,5)P_2, within the PM could also represent cell signals. A crucial question so far remaining unanswered concerns how PtdIns(4,5)P_2 is used by cells to control different physiological processes, for instance exocytosis and endo-

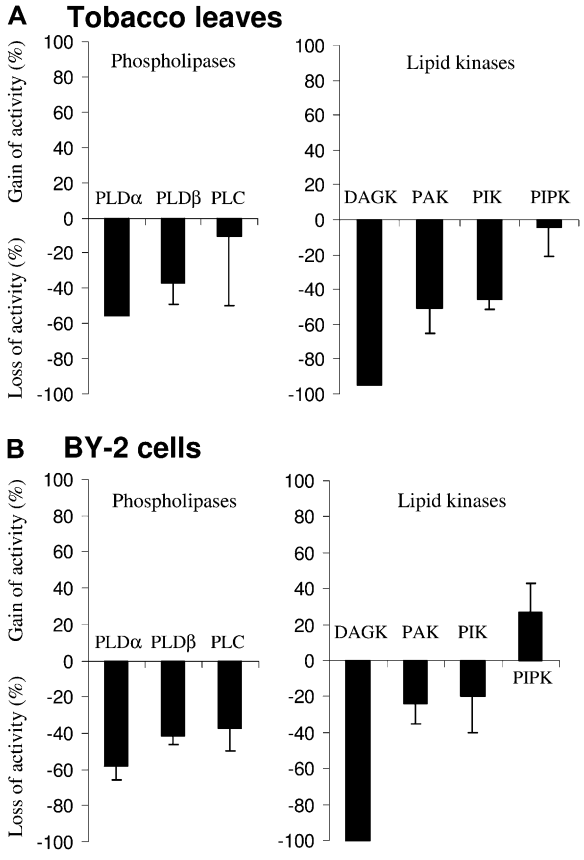

Figure 6. Comparison of specific enzyme activities in C-PM and PM purified from tobacco leaves (A) and BY-2 cells (B). The specific activity of each enzyme was determined in both C-PM and PM as described in "Materials and Methods." The results are expressed as percentage gain or loss of specific activities in C-PM compared with PM. The data are means of three independent experiments ± SD and two independent experiments for DAGK in tobacco leaves and BY-2 cells and for PLD in tobacco leaves.

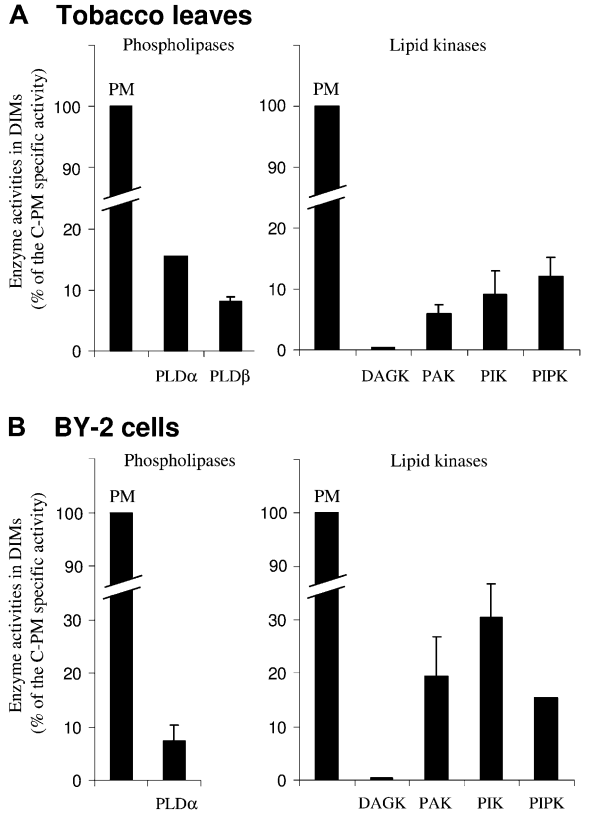

Figure 7. Lipid signaling enzymes are active in DIMs. Comparison of specific enzyme activities in DIMs and C-PM purified from tobacco leaves (A) and BY-2 cells (B). The specific activity of each enzyme was determined in both DIMs and C-PM as described in "Materials and Methods." Enzyme activities in DIMs are expressed as percentages of specific activities in C-PM. The data are means of at least three independent experiments ± SD and two independent experiments for DAGK in tobacco leaves and BY-2 cells, for PLD in tobacco leaves, and for PIPK in BY-2 cells.

cytosis, ion channel and transporter activities, cytoskeletal dynamics, or second messenger production. To this day, our understanding of how local PtdIns(4,5)P_2 concentrations are regulated still remains very limited. The regulatory complexity required for cellular functions is probably achieved by the existence of phospholipid microdomains, such as those analyzed in this study. These domains may serve to properly localize PtdIns(4,5)P_2 as well as to organize PtdIns(4,5)P_2 binding partners into signaling complexes. The hypothesis underlying the work presented here is that the formation of PM microdomains might facilitate the interaction of PtdIns(4,5)P_2 with some binding partners while excluding others. Biochemical studies in animal cells have revealed that about half of cellular PtdIns(4,5)P_2 was recovered in lipid raft-enriched fractions prepared by discontinuous Suc density gradient fractionation (Laux et al., 2000). In this study, we showed, to our knowledge for the first time in plants, that PtdIns(4,5)P_2 is enriched in the DIM fractions isolated from tobacco leaves and BY-2 cells. These results suggest that PtdIns(4,5)P_2-dependent signaling in plants, as well as in animals, could be achieved by its compartmentalization in microdomains.

How Is PtdIns(4,5)P_2 Enriched in Plant MRs?

So far, the mechanisms by which certain lipids, including polyphosphoinositides, are enriched into localized membrane domains as well as the functional significance of their differential distribution between membrane domains (DIMs versus DSMs) remain unclear. Recently, in animal cells, a PtdIns(4,5)P_2-specific phosphatase was targeted to either the raft or nonraft membrane fraction using minimal membrane anchors (Johnson et al., 2008). Targeting of this phosphatase to the nonraft fraction resulted in an enrichment of raft-associated PtdIns(4,5)P_2 and striking changes in cell morphology, including a wortmannin-sensitive increase in cell filopodia and cell spreading. In contrast, the raft-targeted phosphatase depleted the raft pool of PtdIns(4,5)P_2, produced smooth T cells devoid of membrane ruffling and filopodia, and inhibited capping in T cells stimulated by cross-linking the T cell receptor, but without affecting the T cell receptor-dependent calcium flux (Johnson et al., 2008). Another study showed that the expression of type I PtdIns4*P* 5-kinase in mammalian cells increased the number of PtdIns(4,5)P_2 microdomains. Importantly, about half of the PtdIns(4,5)P_2 microdomains were not colocalized with Thy-1, a specific marker of lipid rafts, in spite of the colocalization of transfected PtdIns4*P* 5-kinase with syntaxin clusters (Aoyagi et al., 2005).

In this study, we show that polyphosphoinositides are the only glycerophospholipids enriched in tobacco DIMs. HP-TCL coupled to GC analyses demonstrated that polyphosphoinositides contain predominantly saturated fatty acids. This result is fully consistent with a proposed model by which specific lipids or anchored proteins are selectively recruited into MRs based on their saturated acyl chains (Melkonian et al., 1999). PtdIns, the biosynthetic precursor of PtdIns*P* and PtdIns(4,5)P_2, was largely depleted in DIMs, whereas PtdIns*P* and PtdIns(4,5)P_2 were enriched. From previous studies in plants on the origin of PtdIns, it is clear that its biosynthesis occurs in the endoplasmic reticulum or is associated with the Golgi apparatus (Collin et al., 1999; Lofke et al., 2008), but so far, the mode by which PtdIns is transported to the sites of its further conversion into polyphosphoinositides is unclear. One possible explanation for the lipid distribution patterns observed in tobacco DIMs is that the synthesis of polyphosphoinositides from PtdIns occurs in a nonraft domain and is followed by import into a raft domain. Alternatively, the synthesis of polyphosphoinositides might occur directly inside the raft domain using PtdIns present in small amounts in the raft or a minor pool of PtdIns associated with the rafts that is turned over in its entirety.

In this study, the question of whether polyphosphoinositides are synthesized within or outside the

rafts was challenged by analyzing enzyme activities responsible for their synthesis or degradation. Although no strict enrichment was observed, we were able to detect polyphosphoinositide-synthesizing enzyme activities in tobacco DIMs. One may argue that certain regulators could be lost during the long DIM purification procedure, thus rendering detection of the activity difficult. We could also hypothesize that in contrast to the situation reported for some animal cells, plant MRs do not have a particular enrichment of lipid-modifying enzymes and that polyphosphoinositides are synthesized outside the raft and distribute between DIMs and DSMs afterward, based on their acyl composition and the ensuing biophysical properties of the lipids themselves (Mukherjee et al., 1999; Cho et al., 2006). Indeed, studies on model membranes evidenced that enzymatic phosphorylation of the inositol ring causes insolubility in ordered phospholipid areas and leads to a cooperative reorganization. This strong cooperative effect underlines the important role of PtdIns(4,5)P_2 in signal transduction processes and suggests that the ability of phosphoinositides to induce or reduce long-range interactions in phospholipid mixtures is crucial (Hermelink and Brezesinski, 2008).

Half of PtdIns(4,5)P_2 Is Visualized as Clusters on the Surface of the PM

Controversy raised about the use of mild detergent to purify raft domains has led some authors to propose an artifactual clustering of lipids by detergent treatment (van Rheenen et al., 2005), which may cause ambiguities in the recovery of associated lipids and proteins (Munro, 2003). Nevertheless, many studies provide evidence of strong correlation between experimental results obtained using DIMs and in vivo approaches (Gupta et al., 2006; Raffaele et al., 2009). For instance, the enrichment of PtdIns(4,5)P_2 in raft domains in animal cells has largely been reported (Hope and Pike, 1996; Pike and Casey, 1996; Waugh et al., 1998; Laux et al., 2000), and in particular, caveolae-enriched domains purified without the use of detergent clearly demonstrated an enrichment in PtdIns (4,5)P_2 (Waugh et al., 1998). The GFP-tagged PH domain of PLC that binds to PtdIns(4,5)P_2 in live animal cells (Stauffer et al., 1998; Varnai and Balla, 1998) often showed uneven distributions in the membrane (Botelho et al., 2000; Huang et al., 2004; Aoyagi et al., 2005). However, whether this observation really indicates a local PtdIns(4,5)P_2 accumulation has also been controversial. In contrast, the failure to find a local concentration of PtdIns(4,5)P_2 does not necessarily refute its occurrence but may instead be the result of technical insufficiency. Imaging techniques at the light microscopic level may not have sufficient spatial resolution to detect localized enrichment at a small scale. Indeed, although estimates of the size of lipid domains in animal cells may vary according to the cell type, the physiological status, and the marker used, their reported diameters range from 10 to 200 nm (Simons and Toomre, 2000; Pike, 2006). This small size remains below the classical resolution of confocal microscopy, prompting us to favor an electron microscopy strategy for this investigation. However, electron microscopy is classically used to analyze the distribution of cellular components on sections of biological material but is not immediately suitable to document the spatial distribution of a sparse lipid within the membrane.

In this article, we thus developed a method for the immunological staining of the surface of isolated PM vesicles. This technology has previously been successfully used in a limited number of studies performed on animal and plant cells. It led for instance to the visualization of spatially distinct domains of 60 to 80 nm formed by sphingomyelin and ganglioside M1 (Hullin-Matsuda and Kobayashi, 2007) or to the clustering of Ras molecules in domains of about 50 nm (Prior et al., 2003). A modified version of this method, using freeze-fracture membrane preparation of human fibroblasts, has recently allowed the visualization of PtdIns(4,5)P_2 clusters of 40 to 70 nm in diameter (Fujita et al., 2009), reinforcing previous studies using confocal microscopy that described PtdIns(4,5)P_2 microdomains on the PM of rat cells (Aoyagi et al., 2005). In agreement with these latter studies, the data presented here for tobacco BY-2 cell PM preparations indicate that about 60% of immunodetected PtdIns(4,5)P_2 is observed in clusters of about 25 nm at the PM surface. This observation constitutes, to our knowledge, one of the very first visualizations at the nanoscale level of lipids in plant PM.

Confocal imaging of PtdIns(4,5)P_2 in BY-2 cells, using GFP fused to the PH domain of human PLCδ1, already reported that this lipid was present on the PM but in low amounts, as indicated by the predominant cytosolic localization of the reporter (van Leeuwen et al., 2007). The abundance of gold particles observed at the BY-2 cell PM was rather low (about 160 gold particles per μm^2 of membrane surface), which remains in the same order of magnitude as that found in animal cells (about 400 gold particles per μm^2; Fujita et al., 2009) and is also consistent with the low abundance of PM-associated PtdIns(4,5)P_2 reported by van Leeuwen et al. (2007). Moreover, the proportion of PtdIns(4,5)P_2 visualized as clusters at the PM (about 60%) is very close to the percentage of DIM-associated PtdIns(4,5)P_2 determined in Figure 3 (about 50%). Importantly, the electron microscopy data presented here (Fig. 4) strengthen the evidence of a lateral segregation of this lipid within the PM and rule out the hypothesis of an artifactual aggregation during DIM isolation, since the electron microscopy methodology employed does not require any fixation procedure, susceptible to induce artificial clustering.

PtdIns(4,5)P_2 PM Clustering Is Not Sterol Dependent

Another important aspect to be considered is presented by the interactions of raft-constituting lipid classes, and the question has been raised of their

respective roles in the organization of MR domains. Animal and plant DIMs are both enriched in sterols. It has already been shown that free sterols serve as molecular spacers, filling voids between associated sphingolipids, and interact preferentially with sphingolipids due to the saturation of the associated hydrocarbon chains (Binder et al., 2003). Moreover, sterol modifies the physical state of membranes, because of the conformational inflexibility of its steroid ring system. In a lipid bilayer, cholesterol orients parallel to the lipid hydrocarbon chains, with its hydrophobic moiety inside the membrane and its polar 3-OH toward the lipid-water interface (Binder et al., 2003). Sterols have previously been suggested to be responsible for the clustering of lipid and protein components of MRs. In a former study, we have demonstrated that treatment of BY-2 cell PM with the free sterol chelator mbCD led to a drastic depletion of the PM sterol content (about 50%) without affecting either the phospholipid or the protein association with the PM (Roche et al., 2008). In this study, a similar treatment of the PM with mbCD did not affect the density of gold particles corresponding to antibodies to PtdIns(4,5)P_2. Similar results have been obtained in several other studies, and the density of labeling observed at the PM surface was not decreased by mbCD treatment either in the case of ganglioside M1 on mouse fibroblast membranes (Fujita et al., 2007) or with a raft marker protein such as the C terminus of a Ras protein fused to GFP (Parton and Hancock, 2004). A slight increase of the labeling corresponding to PtdIns(4,5)P_2 was even observed on freeze fracture replica of human fibroblasts after mbCD treatment (Fujita et al., 2009). These results are in perfect agreement with the work presented here, suggesting that the association of this lipid with the PM is not sterol dependent.

Moreover, the results presented here indicate that the mbCD treatment does not significantly modify the proportion of PtdIns(4,5)P_2 molecules observed in clusters. Among the few references reporting the effect of sterol depletion on the visualization of clustered membrane components, results are at variance. The clustering of ganglioside M1 on the PM of mouse fibroblast was only partially affected by a mbCD treatment (Fujita et al., 2007). Another study indicated that the clustering of GFP fused to the minimal PM-targeting motifs of H-Ras was completely abolished by the same treatment, whereas the clustering of full-length H-Ras was only slightly affected in the same conditions (Prior et al., 2003). The distribution in clusters of mouse node cell PM proteins was not modified by mbCD treatment (Lillemeier et al., 2006). Finally, the clustering of PtdIns(4,5)P_2 on human dermal fibroblasts was only slightly affected by mbCD.

The observation that the location of saturated polyphosphoinositides was independent of the presence of cholesterol may reflect another kind of interaction between polyphosphoinositides and raft lipids and proteins. In good agreement, the observed phase separation of the highly charged PtdIns(4,5)P_2 is presumably water stabilized by electrostatic interactions and hydrogen bonding (Levental et al., 2008). Indeed, structural and functional studies of lateral heterogeneity in biological membranes have underlined the importance of steric determinants for membrane organization, such as head group size and acyl chain saturation, and the significant electrostatic contributions. For molecules with steric cross-sections typical of phospholipids in the cell membrane, only polyphosphoinositides fulfill the requirements for lipids with substantial effects on membrane organization. PtdIns(4,5)P_2 contains between three and four negative charges at physiological conditions. Theory and experiment show that membrane surface pressure increases linearly with PtdIns(4,5)P_2 net charge and reveal crossing of high- and low-ionic-strength pressure-area isotherms, due to opposing effects of ionic strength in compressed and expanded monolayers (Levental et al., 2008). Thus, the appearance of MR domains in the PM could be explained solely based on the biophysical properties of the lipid phase constituting the membrane for review (Binder et al., 2003).

Plant MRs as Polyphosphoinositide-Enriched Signaling Platforms

Previous observations have shown that stress-induced polyphosphoinositide species differed in their fatty acid composition from polyphosphoinositides that are constitutively present in plant cell membranes (Konig et al., 2008b). Because the data presented in this study indicate that polyphosphoinositides associated with MRs are highly saturated (Fig. 2), it might be concluded that stress-induced, unsaturated polyphosphoinositides might not be associated with DIMs. It is possible that physiological roles of stress-induced polyphosphoinositides exceed those of constitutive species, which would be consistent with a functional distinction of polyphosphoinositides associated with DIMs versus those in DSMs. So far, there is little evidence to support or refute this concept. The results reported here suggest that in resting plant cells, not challenged by stimulation, the activities of several lipid signaling-related enzymes were present at low levels in tobacco DIMs (ranging from 8% to 25% of specific activity compared with C-PM). One can hypothesize that stimulation might change this pattern and that activation of lipid signaling-related enzymes occurs in DIMs. For instance, PLDα or PLDβ activities, which were detected at low levels in plant DIMs, might be activated within DIMs, as has been demonstrated in animal cells where PLD activities measured in DIMs are low in nonstimulated cells unless challenged by G-protein activator (Bychenok and Foster, 2000; Xu et al., 2000; Diaz et al., 2002). In another study, PLC1 was not detected by western blot in DIMs purified from T cells (Veri et al., 2001). In the work presented here, it is possible that the variability observed in the PLC activity detected in tobacco DIMs is related to labile association of this enzyme with the membrane.

Concerning DAG kinase, its activity was measured in freshly prepared PM but was extremely sensitive to the DIM purification procedure, and no activity was detected in the DIM fraction. Although similar results were obtained in DIM purified from Madin-Darby canine kidney cells (Hope and Pike, 1996), it might be hypothesized that the strong reduction in DIM-associated DAG kinase activity is an artifact of the lengthy preparation procedures rather than a true reflection of its distribution.

While not strictly enriched, PtdOH kinase activity was detected in DIMs at approximately 20% of specific activity of the PM in BY-2 cells. Interestingly, PtdOH kinase was able to phosphorylate endogenous PtdOH to DGPP in DIM fractions in the absence of exogenous PtdOH (data not shown), suggesting the presence of endogenous PtdOH in DIMs available for phosphorylation. DGPP synthesized by this not-yet-cloned PtdOH kinase is a second messenger likely involved in many signaling events in plants, such as cell responses upon treatment with a hormone or an elicitor of the defense reaction (Pical et al., 1999; Munnik et al., 2000; Zalejski et al., 2005, 2006). Whether the presence of PtdOH kinase might support a role for lateral segregation of lipids and proteins in the membrane, or might be involved in the plant signaling pathway, are current questions studied in our laboratories.

In summary, we could demonstrate that DIM fractions isolated from plant PMs contain an enriched proportion of saturated polyphosphoinositides, including PtdIns4*P* and PtdIns(4,5)P_2. The biochemical data are supported by electron micrographs showing localized clustering of PtdIns(4,5)P_2 in the plane of the PM of plant cells, correlating biochemical data and imaging. A detailed analysis of DIMs and C-PMs of nonstressed cells for enzyme activities involved in polyphosphoinositide biosynthesis or breakdown indicates that DIMs contain a complement of relevant enzymes, although without substantial enrichment. While such analyses are pushing the limits of experimental accessibility, and the question of the origin of DIM-associated polyphosphoinositides must remain speculative at this point, our data provide several lines of evidence for the existence of polyphosphoinositide-containing microdomains in plant PMs. Future experiments will be directed toward elucidating the functional relevance of different polyphosphoinositide species present in DIM or DSM fractions of plant PM. Further progress requires an improved understanding of the relevant lipid kinases and phosphatases, how they are regulated, where they are localized in cells, and with which partner proteins they might colocalize and functionally interact.

MATERIALS AND METHODS

Plant Materials

Leaves were obtained from 8-week-old tobacco plants (*Nicotiana tabacum* 'Xanthi') grown in a growth chamber at 25°C under 16/8-h day/night conditions. Wild-type BY-2 cells (cv Bright Yellow 2) were grown as described previously (Morel et al., 2006).

Preparation and Purity of Tobacco PM

All steps were performed at 4°C. PMs were obtained after cell fractionation according to Mongrand et al. (2004) by partitioning in an aqueous polymer two-phase system with polyethylene glycol 3350/dextran T-500 (6.6% each). Protein amounts were determined according to Bradford (1976) using bovine serum albumin as a standard. PMs were treated with 1% (w/w) TX100 for 30 min at 4°C. After solubilization, membranes were brought to a 52% (w/w) final concentration of Suc, overlaid with 3 mL of 35%, 30%, and 5% (w/w) Suc in Tris-buffered saline (TBS) buffer, and then spun for 16 h at 150,000*g* at 4°C in a TST41 rotor (Sorvall). DIMs were recovered below the 30% to 35% layers and washed in 4 mL of TBS buffer to remove residual Suc. The protein concentration was determined with the Bio-Rad protein assay kit (bicinchoninic acid) to avoid TX100 interference, using bovine serum albumin as a protein standard. All buffers were ice cold, and the final recovering buffer contained the following protease inhibitors: 0.5 mg mL^{-1} leupeptin, 0.7 mg mL^{-1} pepstatin, and 0.2 mM phenylmethylsulfonyl fluoride.

Analysis of Lipids by HP-TLC and Quantification

Lipids were extracted according to Mongrand et al. (2004) and Lefebvre et al. (2007). Polyphosphoinositides were extracted from PM and DIMs using an acidic extraction protocol (Konig et al., 2007). Lipids were separated by TLC on silica gel plates (HP-TLC silicagel 60F 254; Merck) using developing solvents for optimal resolution: for polyphosphoinositides and PtdOH, $CHCl_3$:CH_3OH:NH_4OH:water (57:50:4:11, v/v/v/v); for PtdCho and PtdEtn, acetone:toluol:water (91:30:7, v/v/v); for isolating PtdIns, $CHCl_3$:methyl acetate:isopropanol:CH_3OH:0.25% aqueous potassium chloride (25:25:25:10:9, v/v/v/v/v). Lanes with authentic lipid standards (5 μg; Aventi Polar Lipids) run in parallel with biological samples were cut, and lipids were visualized in aqueous 10% (w/w) $CuSO_4$ (Sigma) containing 8% (w/v) H_3PO_4 (Sigma) and subsequent heating to 180°C. Unstained lipids were located on the remaining parts of the TLC plates, according to standard migration, scraped, redissolved in their respective developing solvents, and dried under N_2 flow. Lipids were transmethylated (Konig et al., 2007), and fatty acid methyl esters were dissolved in acetonitrile and analyzed using a GC6890 gas chromatograph with flame-ionization detection (Agilent) fitted with a 30-m × 250-μm DB-23 capillary column (Agilent). Helium flowed as a carrier gas at 1 mL min^{-1}. Samples were injected at 220°C. After 1 min at 150°C, the oven temperature was raised to 200°C at a rate of 8°C min^{-1}, then to 250°C at 25°C min^{-1}, and then kept at 250°C for 6 min. Fatty acids were identified according to authentic standards and by their characteristic mass spectrometric fragmentation patterns (data not shown) and quantified according to internal tripentadecanoic acid standards of known concentration. Variation in fatty acid patterns obtained with material sampled on different days did not exceed that denoted by SD. Due to limiting material in samples representing isolated minor lipids, fatty acids of low abundance may be absent from fatty acid patterns.

Lipid Dot Blot and Immunodetection

The immunodetection of PtdIns(4,5)P_2 was performed according to Diaz et al. (2002). Briefly, lipids solubilized in TBS supplemented with 0.05% (v/v) Tween 20 (TBS-T) or PM/DIMs purified from BY-2 cells were dotted on polyscreen PVDF membranes using a Bio-Dot SF apparatus (Bio-Rad). Membranes were rinsed with distilled water and blocked with 5% (w/v) bovine serum albumin in TBS-T for 2 h. Membranes were then incubated with the monoclonal mouse antibody against native PtdIns(4,5)P_2 from bovine spinal cord (www.assay designs.com) in TBS-T containing 5% bovine serum albumin overnight at 4°C. After two 20-min washes with TBS-T, membranes were incubated with horseradish peroxidase-conjugated secondary antibody in TBS-T containing 5% (w/v) bovine serum albumin for 1 h, rinsed two times for 30 min with TBS-T, and developed with the enhanced chemiluminescence reagent (Perkin-Elmer).

Immunogold Labeling of Purified Plant Membranes

Purified BY-2 cell PM vesicles were directly deposited onto collodion-coated and carbon-stabilized microscope grids. For each grid, a deposit of 10 μL of an optimum concentration of 0.2 $\mu g\ \mu L^{-1}$ purified PM was previously determined to allow a convenient spreading of the vesicles onto the grid surface. The grids were then floated, at room temperature, on 20-μL droplets

of successive incubating solutions: (1) 20 min with a 5% (w/w) blocking solution of heat-inactivated normal goat serum plus 0.1% (w/w) Gly and 0.1% (w/w) dried milk in 20 mM TBS, pH 7.4; (2) 45 min with a primary antibody diluted in TBS containing 0.1% of the blocker protein: rabbit polyclonal primary antibodies to REM α130 (Raffaele et al., 2009) were diluted 1:800 and a mouse monoclonal antibody against PtdIns(4,5)P_2 and antibody against native PtdIns(4,5)P_2 from bovine spinal cord (www.assay designs.com) was diluted 10 times; (3) 45 min with a goat anti-rabbit IgG conjugate (EM GAR 10 nm; British Biocell International) labeled to 10-nm colloidal gold particles or goat anti-mouse IgG conjugate (EM GAM 5 nm; British Biocell International) labeled to 5-nm colloidal gold particles. After this immunolabeling, a fixation step was performed in 0.5% (w/v) glutaraldehyde in 0.1 M Sorensen's phosphate buffer. After washes in the same buffer, preparations were negatively stained in 1% (w/v) ammonium molybdate (1 min at room temperature) and air dried. Grids were observed with a Hitachi H7500 transmission electron microscope operating at 80 kV equipped with an AMT camera driven by AMT software.

Depletion of free sterols of PM purified fraction was performed by incubating fresh purified PM with 20 mM mbCD for 30 min at room temperature with stirring, according to Roche et al. (2008). Control experiments were performed to confirm the specificity of the labeling: omission of the primary antibody incubation step for both REM and PtdIns(4,5)P_2 immunocytological assays, and use of preimmune IgG instead of REM primary antibody (Supplemental Fig. S4). Measure of each vesicle surface exhibiting some labeling was estimated using ImageJ as well as the number of gold particles per vesicle, allowing the determination of the density of gold particles per μm^2 of isolated vesicle visualized. Distances between gold particles were recorded with the AMT software. Measures were carried out on at least 30 images per independent experiment, and three independent biochemical PM purifications from BY-2 cells were performed. The first experiment allowed us to determine the optimized conditions of immunolabeling for the detection of PtdIns(4,5)P_2 and to prove that only one freeze-thaw cycle (−80°C) of the MP vesicles could preserve antigenic sites for an efficient immunolabeling. For each experiment, we observed six replicates of immunolabeling and two replicates of each control sample.

Measurement of Enzymatic Activities

To avoid a lack of reproducibility, great care was taken to use only freshly prepared membranes (PM, C-PM, DIM), because we observed that freeze/thaw cycles of membranes greatly impaired our measurement.

PLDα activities were assayed as described previously with modifications (Ritchie and Gilroy, 1998). Vesicles of PtdCho were prepared mixing PtdCho and [^{14}C]PtdCho in a molar ratio of 40:0.5. Organic solvents were dried under streaming nitrogen, and lipids were resuspended in 10 μL of reaction buffer (50 mM MES, pH 6.5, 1.25 mM $CaCl_2$, 5 mM $MgCl_2$, and 50 μM SDS) to 400 μM final concentration and sonicated for 15 min at 4°C. Membrane fractions containing 2 μg of proteins were incubated for 30 min at 30°C with vesicles of PtdCho in the presence of 1% (v/v) butanol in a final volume of 100 μL. Reactions were stopped with 375 μL of $CHCl_3$:CH_3OH (2:1, v/v). Equal volumes (100 μL) of $CHCl_3$ and 2 M KCl were added sequentially to generate a two-phase system. After mixing and centrifugation at 12,000g for 5 min, the organic phase was dried under gaseous nitrogen. Lipids were resuspended in 40 μL of $CHCl_3$:CH_3OH (2:1, v/v) mixture, spotted on silica plates (HP-TLC silicagel 60F 254; Merck), and developed with methyl acetate:*n*-propanol:$CHCl_3$:CH_3OH:0.25% KCl (25:25:25:10:9, v/v/v/v/v). Radiolabeled phosphatidylbutanol was visualized using a phosphor imager and quantified using the [^{14}C]PtdCho calibration curve.

PLDβ activities were measured according to Novotna et al. (2003). Lipids {PtdEtn:PtdIns(4,5)P_2:PtdCho:[^{14}C]PtdCho} were mixed in a 36:3.2:2.2:0.5 molar ratio. Organic solvents were dried under gaseous nitrogen, and lipids were resuspended in 10 μL of reaction buffer (0.1 M MES, pH 6.8, 100 μM $CaCl_2$, 2 mM $MgCl_2$, 80 mM KCl, and 0.1% [v/v] TX100) to 420 μM final concentration and sonicated for 15 min at 4°C. Membrane fractions containing 5 μg of proteins were incubated for 30 min at 30°C with lipids in the presence of 1% (v/v) butanol in a 100-μL final volume. Reactions were stopped, and lipids were extracted and analyzed as described previously.

Lipid kinases activities were assayed essentially according to Kamada and Muto (1991), except for PtdOH kinase activity (Wissing et al., 1994). To assay DAG kinase, lipids (10 μg of DAG and 40 μg of phosphatidylglycerol) were mixed, dried under gaseous nitrogen, and resuspended in 10 μL of reaction buffer (50 mM Tris-HCl, pH 7.5, 10 mM $MgCl_2$, 0.02% [v/v] TX100, 1 mM dithiothreitol [DTT], and 3 mM CHAPS). Membrane fractions containing 5 μg of proteins were incubated for 5 min at 30°C with lipids and [γ-^{32}P]ATP (5 μCi, 3,000 Ci mmol^{-1}) in a 50-μL final reaction volume. To measure PtdOH kinase activity, PtdOH (20 μg) was mixed, dried under gaseous nitrogen, resuspended in 10 μL of reaction buffer (40 mM imidazole, pH 6.1, 10 mM $MgCl_2$, 100 mM NaCl, 0.1 mM EDTA, 3.5 mM β-mercaptoethanol, and 3 mM TX100), and sonicated for 15 min. Membrane fractions containing 5 μg of proteins were incubated for 5 min at 30°C with PtdOH and [γ-^{32}P]ATP (5 μCi, 3,000 Ci mmol^{-1}) in a 50-μL final reaction volume. To assay PtdIns kinase activity, PtdIns (20 μg) was mixed, dried under gaseous nitrogen, resuspended in 10 μL of reaction buffer (50 mM Tris-HCl, pH 7.5, 10 mM $MgCl_2$, 5 mM EGTA, and 1 mM DTT), and sonicated for 15 min. Membrane fractions containing 5 μg of proteins were incubated for 5 min at 30°C in the presence of PtdIns and [γ-^{32}P]ATP (5 μCi, 3,000 Ci mmol^{-1}) in a 50-μL final reaction volume. To measure PtdIns*P* kinase activity, membrane fractions containing 1 μg of proteins were incubated for 5 min at 30°C in 50 μL of reaction buffer (50 mM Tris-HCl, pH 7.5, 10 mM $MgCl_2$, 5 mM EGTA, 1 mM DTT, and 0.06% [v/v] TX100) in the presence of [γ-^{32}P]ATP (5 μCi, 3,000 Ci mmol^{-1}), and 5 μg of PtdIns4*P* was added in micellar form. Lipid kinases reactions were stopped by the addition of 180 μL of $CHCl_3$:CH_3OH:HCl (100:50:1, v/v/v), 50 μL of chloroform, and 50 μL of 9‰ NaCl. After vortexing and centrifugation at 12,000g for 5 min, radiolabeled lipids present in organic phases were spotted on silica plates (HP-TLC silicagel 60F 254; Merck), developed with chloroform:methanol:25% NH_4:water (45:35:2:8, v/v/v/v), visualized, and quantified with a phosphor imager.

PLC activities were measured as described previously (Melin et al., 1987). Lipids {0.01 μmol of PtdIns(4,5)P_2 and 0.02 μCi of [inositol-2-^{3}H(N)]PtdIns(4,5)P_2, 6.8 mCi mmol^{-1}} were mixed, dried under gaseous nitrogen, resuspended in water to 1 mM final concentration, and sonicated for 15 min at 4°C. Assays (50 μL) containing 50 mM Tris-HCl, pH 6.6, 1 μM free calcium, lipids, and 10 μg of proteins of the different membrane fractions were run for 20 min at 30°C. Reactions were stopped with 1 mL of cold $CHCl_3$:CH_3OH (2:1, v/v). After the addition of 250 μL of cold 1 N HCl, the mixtures were vortexed and centrifuged at 12,000g for 5 min. A total of 200 μL of the aqueous phases containing the radiolabeled reaction products was collected and analyzed by liquid scintillation counting (1600 TR; Packard).

Supplemental Data

The following materials are available in the online version of this article.

Supplemental Figure S1. Determination of the initial velocity of each enzyme.

Supplemental Figure S2. Determination of the activity of each enzyme according to the amount of proteins.

Supplemental Figure S3. The PtdIns kinase activity present in tobacco PM is a type III PtdIns 4-kinase.

Supplemental Figure S4. Controls for electron microscopy and immunogold labeling controls of negatively stained tobacco PM vesicles for REM and PtdIns(4,5)P_2.

Supplemental Figure S5. Cross-reactivity of antibodies against PtdIns(4,5)P_2.

Received October 21, 2009; accepted February 12, 2010; published February 24, 2010.

LITERATURE CITED

Aoyagi K, Sugaya T, Umeda M, Yamamoto S, Terakawa S, Takahashi M (2005) The activation of exocytotic sites by the formation of phosphatidylinositol 4,5-bisphosphate microdomains at syntaxin clusters. J Biol Chem **280:** 17346–17352

Bhat RA, Miklis M, Schmelzer E, Schulze-Lefert P, Panstruga R (2005) Recruitment and interaction dynamics of plant penetration resistance components in a plasma membrane microdomain. Proc Natl Acad Sci USA **102:** 3135–3140

Bhat RA, Panstruga R (2005) Lipid rafts in plants. Planta **223:** 5–19

Binder WH, Barragan V, Menger FM (2003) Domains and rafts in lipid membranes. Angew Chem Int Ed Engl **42:** 5802–5827

Bohn M, Heinz E, Luthje S (2001) Lipid composition and fluidity of plasma membranes isolated from corn (Zea mays L.) roots. Arch Biochem Biophys **387:** 35–40

Borner GH, Sherrier DJ, Weimar T, Michaelson LV, Hawkins ND, Macaskill A, Napier JA, Beale MH, Lilley KS, Dupree P (2005) Analysis of detergent-resistant membranes in Arabidopsis: evidence for plasma membrane lipid rafts. Plant Physiol **137:** 104–116

Botelho RJ, Teruel M, Dierckman R, Anderson R, Wells A, York JD, Meyer T, Grinstein S (2000) Localized biphasic changes in phosphatidylinositol-4,5-bisphosphate at sites of phagocytosis. J Cell Biol **151:** 1353–1368

Bradford MM (1976) A rapid and sensitive method for the quantitation of microgram quantities of protein utilizing the principle of protein-dye binding. Anal Biochem **72:** 248–254

Braun M, Baluska F, von Witsch M, Menzel D (1999) Redistribution of actin, profilin and phosphatidylinositol-4,5-bisphosphate in growing and maturing root hairs. Planta **209:** 435–443

Brown DA (2006) Lipid rafts, detergent-resistant membranes, and raft targeting signals. Physiology (Bethesda) **21:** 430–439

Brown DA, London E (2000) Structure and function of sphingolipid- and cholesterol-rich membrane rafts. J Biol Chem **275:** 17221–17224

Bychenok S, Foster DA (2000) A low molecular weight factor from dividing cells activates phospholipase D in caveolin-enriched membrane microdomains. Arch Biochem Biophys **377:** 139–145

Cho H, Kim YA, Ho WK (2006) Phosphate number and acyl chain length determine the subcellular location and lateral mobility of phosphoinositides. Mol Cells **22:** 97–103

Collin S, Justin AM, Cantrel C, Arondel V, Kader JC (1999) Identification of AtPIS, a phosphatidylinositol synthase from Arabidopsis. Eur J Biochem **262:** 652–658

DeWald DB, Torabinejad J, Jones CA, Shope JC, Cangelosi AR, Thompson JE, Prestwich GD, Hama H (2001) Rapid accumulation of phosphatidylinositol 4,5-bisphosphate and inositol 1,4,5-trisphosphate correlates with calcium mobilization in salt-stressed Arabidopsis. Plant Physiol **126:** 759–769

Diaz O, Berquand A, Dubois M, Di Agostino S, Sette C, Bourgoin S, Lagarde M, Nemoz G, Prigent AF (2002) The mechanism of docosahexaenoic acid-induced phospholipase D activation in human lymphocytes involves exclusion of the enzyme from lipid rafts. J Biol Chem **277:** 39368–39378

Di Paolo G, De Camilli P (2006) Phosphoinositides in cell regulation and membrane dynamics. Nature **443:** 651–657

Fujita A, Cheng J, Hirakawa M, Furukawa K, Kusunoki S, Fujimoto T (2007) Gangliosides GM1 and GM3 in the living cell membrane form clusters susceptible to cholesterol depletion and chilling. Mol Biol Cell **18:** 2112–2122

Fujita A, Cheng J, Tauchi-Sato K, Takenawa T, Fujimoto T (2009) A distinct pool of phosphatidylinositol 4,5-bisphosphate in caveolae revealed by a nanoscale labeling technique. Proc Natl Acad Sci USA **106:** 9256–9261

Gupta N, Wollscheid B, Watts JD, Scheer B, Aebersold R, DeFranco AL (2006) Quantitative proteomics analysis of B cell lipid rafts reveals that ezrin regulates antigen receptor-mediated lipid rafts dynamics. Nat Immunol **7:** 625–633

Hegewald H (1996) One-dimensional thin-layer chromatography of all known D-3 and D-4 isomers of phosphoinositides. Anal Biochem **242:** 152–155

Heilmann I (2009) Using genetic tools to understand plant phosphoinositide signalling. Trends Plant Sci **14:** 171–179

Hermelink A, Brezesinski G (2008) Do unsaturated phosphoinositides mix with ordered phosphadidylcholine model membranes? J Lipid Res **49:** 1918–1925

Hope HR, Pike LJ (1996) Phosphoinositides and phosphoinositide-utilizing enzymes in detergent-insoluble lipid domains. Mol Biol Cell **7:** 843–851

Huang S, Lifshitz L, Patki-Kamath V, Tuft R, Fogarty K, Czech MP (2004) Phosphatidylinositol-4,5-bisphosphate-rich plasma membrane patches organize active zones of endocytosis and ruffling in cultured adipocytes. Mol Cell Biol **24:** 9102–9123

Hullin-Matsuda F, Kobayashi T (2007) Monitoring the distribution and dynamics of signaling microdomains in living cells with lipid-specific probes. Cell Mol Life Sci **64:** 2492–2504

Johnson CM, Chichili GR, Rodgers W (2008) Compartmentalization of phosphatidylinositol 4,5-bisphosphate signaling evidenced using targeted phosphatases. J Biol Chem **283:** 29920–29928

Jung JY, Kim YW, Kwak JM, Hwang JU, Young J, Schroeder JI, Hwang I, Lee Y (2002) Phosphatidylinositol 3- and 4-phosphate are required for normal stomatal movements. Plant Cell **14:** 2399–2412

Kamada Y, Muto S (1991) Ca^{2+} regulation of phosphatidylinositol turnover in the plasma membrane of tobacco suspension culture cells. Biochim Biophys Acta **1093:** 72–79

Konig S, Hoffmann M, Mosblech A, Heilmann I (2008a) Determination of content and fatty acid composition of unlabeled phosphoinositide species by thin-layer chromatography and gas chromatography. Anal Biochem **378:** 197–201

Konig S, Ischebeck T, Lerche J, Stenzel I, Heilmann I (2008b) Salt-stress-induced association of phosphatidylinositol 4,5-bisphosphate with clathrin-coated vesicles in plants. Biochem J **415:** 387–399

Konig S, Mosblech A, Heilmann I (2007) Stress-inducible and constitutive phosphoinositide pools have distinctive fatty acid patterns in Arabidopsis thaliana. FASEB J **21:** 1958–1967

Kost B, Lemichez E, Spielhofer P, Hong Y, Tolias K, Carpenter C, Chua NH (1999) Rac homologues and compartmentalized phosphatidylinositol 4,5-bisphosphate act in a common pathway to regulate polar pollen tube growth. J Cell Biol **145:** 317–330

Laux T, Fukami K, Thelen M, Golub T, Frey D, Caroni P (2000) GAP43, MARCKS, and CAP23 modulate PI(4,5)P(2) at plasmalemmal rafts, and regulate cell cortex actin dynamics through a common mechanism. J Cell Biol **149:** 1455–1472

Lee Y, Kim YW, Jeon BW, Park KY, Suh SJ, Seo J, Kwak JM, Martinoia E, Hwang I (2007) Phosphatidylinositol 4,5-bisphosphate is important for stomatal opening. Plant J **52:** 803–816

Lefebvre B, Furt F, Hartmann MA, Michaelson LV, Carde JP, Sargueil-Boiron F, Rossignol M, Napier JA, Cullimore J, Bessoule JJ, et al (2007) Characterization of lipid rafts from *Medicago truncatula* root plasma membranes: a proteomic study reveals the presence of a raft-associated redox system. Plant Physiol **144:** 402–418

Levental I, Janmey PA, Cebers A (2008) Electrostatic contribution to the surface pressure of charged monolayers containing polyphosphoinositides. Biophys J **95:** 1199–1205

Lillemeier BF, Pfeiffer JR, Surviladze Z, Wilson BS, Davis MM (2006) Plasma membrane-associated proteins are clustered into islands attached to the cytoskeleton. Proc Natl Acad Sci USA **103:** 18992–18997

Liu K, Li L, Luan S (2005) An essential function of phosphatidylinositol phosphates in activation of plant shaker-type K^+ channels. Plant J **42:** 433–443

Lofke C, Ischebeck T, Konig S, Freitag S, Heilmann I (2008) Alternative metabolic fates of phosphatidylinositol produced by phosphatidylinositol synthase isoforms in Arabidopsis thaliana. Biochem J **413:** 115–124

Meijer HJ, Munnik T (2003) Phospholipid-based signaling in plants. Annu Rev Plant Biol **54:** 265–306

Melin PM, Sommarin M, Sandelius AS, Jergil B (1987) Identification of Ca^{2+}-stimulated polyphosphoinositide phospholipase C in isolated plant plasma membranes. FEBS Lett **223:** 87–91

Melkonian KA, Ostermeyer AG, Chen JZ, Roth MG, Brown DA (1999) Role of lipid modifications in targeting proteins to detergent-resistant membrane rafts: many raft proteins are acylated, while few are prenylated. J Biol Chem **274:** 3910–3917

Metcalf TN III, Villanueva MA, Schindler M, Wang JL (1986) Monoclonal antibodies directed against protoplasts of soybean cells: analysis of the lateral mobility of plasma membrane-bound antibody MVS-1. J Cell Biol **102:** 1350–1357

Mongrand S, Morel J, Laroche J, Claverol S, Carde JP, Hartmann MA, Bonneu M, Simon-Plas F, Lessire R, Bessoule JJ (2004) Lipid rafts in higher plant cells: purification and characterization of Triton X-100-insoluble microdomains from tobacco plasma membrane. J Biol Chem **279:** 36277–36286

Monteiro D, Castanho Coelho P, Rodrigues C, Camacho L, Quader H, Malho R (2005a) Modulation of endocytosis in pollen tube growth by phosphoinositides and phospholipids. Protoplasma **226:** 31–38

Monteiro D, Liu Q, Lisboa S, Scherer GE, Quader H, Malho R (2005b) Phosphoinositides and phosphatidic acid regulate pollen tube growth and reorientation through modulation of $[Ca^{2+}]c$ and membrane secretion. J Exp Bot **56:** 1665–1674

Morel J, Claverol S, Mongrand S, Furt F, Fromentin J, Bessoule JJ, Blein JP, Simon-Plas F (2006) Proteomics of plant detergent-resistant membranes. Mol Cell Proteomics **5:** 1396–1411

Mueller-Roeber B, Pical C (2002) Inositol phospholipid metabolism in Arabidopsis: characterized and putative isoforms of inositol phospho-

lipid kinase and phosphoinositide-specific phospholipase C. Plant Physiol **130:** 22–46

Mukherjee S, Soe TT, Maxfield FR (1999) Endocytic sorting of lipid analogues differing solely in the chemistry of their hydrophobic tails. J Cell Biol **144:** 1271–1284

Munnik T, Meijer HJ, Ter Riet B, Hirt H, Frank W, Bartels D, Musgrave A (2000) Hyperosmotic stress stimulates phospholipase D activity and elevates the levels of phosphatidic acid and diacylglycerol pyrophosphate. Plant J **22:** 147–154

Munnik T, Testerink C (2009) Plant phospholipid signaling: "in a nutshell". J Lipid Res (Suppl) **50:** S260–S265

Munro S (2003) Lipid rafts: elusive or illusive? Cell **115:** 377–388

Novotna Z, Martinec J, Profotova B, Zdarova S, Kader JC, Valentova O (2003) In vitro distribution and characterization of membrane-associated PLD and PI-PLC in Brassica napus. J Exp Bot **54:** 691–698

Parton RG, Hancock JF (2004) Lipid rafts and plasma membrane microorganization: insights from Ras. Trends Cell Biol **14:** 141–147

Pical C, Westergren T, Dove SK, Larsson C, Sommarin M (1999) Salinity and hyperosmotic stress induce rapid increases in phosphatidylinositol 4,5-bisphosphate, diacylglycerol pyrophosphate, and phosphatidylcholine in Arabidopsis thaliana cells. J Biol Chem **274:** 38232–38240

Pike LJ (2006) Rafts defined: a report on the Keystone Symposium on Lipid Rafts and Cell Function. J Lipid Res **47:** 1597–1598

Pike LJ, Casey L (1996) Localization and turnover of phosphatidylinositol 4,5-bisphosphate in caveolin-enriched membrane domains. J Biol Chem **271:** 26453–26456

Prior IA, Muncke C, Parton RG, Hancock JF (2003) Direct visualization of Ras proteins in spatially distinct cell surface microdomains. J Cell Biol **160:** 165–170

Raffaele S, Bayer E, Lafarge D, Cluzet S, German Retana S, Boubekeur T, Leborgne-Castel N, Carde JP, Lherminier J, Noirot E, et al (2009) Remorin, a Solanaceae protein resident in membrane rafts and plasmodesmata, impairs potato virus X movement. Plant Cell **21:** 1541–1555

Rajendran L, Simons K (2005) Lipid rafts and membrane dynamics. J Cell Sci **118:** 1099–1102

Ritchie S, Gilroy S (1998) Abscisic acid signal transduction in the barley aleurone is mediated by phospholipase D activity. Proc Natl Acad Sci USA **95:** 2697–2702

Roche Y, Gerbeau-Pissot P, Buhot B, Thomas D, Bonneau L, Gresti J, Mongrand S, Perrier-Cornet JM, Simon-Plas F (2008) Depletion of phytosterols from the plant plasma membrane provides evidence for disruption of lipid rafts. FASEB J **22:** 3980–3991

Simons K, Toomre D (2000) Lipid rafts and signal transduction. Nat Rev Mol Cell Biol **1:** 31–39

Stanislas T, Bouyssie D, Rossignol M, Vesa S, Fromentin J, Morel J, Pichereaux C, Monsarrat B, Simon-Plas F (2009) Quantitative proteomics reveals a dynamic association of proteins to detergent-resistant membranes upon elicitor signaling in tobacco. Mol Cell Proteomics **8:** 2186–2198

Stauffer TP, Ahn S, Meyer T (1998) Receptor-induced transient reduction in plasma membrane PtdIns(4,5)P2 concentration monitored in living cells. Curr Biol **8:** 343–346

Stevenson JM, Perera IY, Heilmann II, Persson S, Boss WF (2000) Inositol signaling and plant growth. Trends Plant Sci **5:** 357

van Leeuwen W, Vermeer JE, Gadella TW Jr, Munnik T (2007) Visualization of phosphatidylinositol 4,5-bisphosphate in the plasma membrane of suspension-cultured tobacco BY-2 cells and whole Arabidopsis seedlings. Plant J **52:** 1014–1026

van Rheenen J, Achame EM, Janssen H, Calafat J, Jalink K (2005) PIP2 signaling in lipid domains: a critical re-evaluation. EMBO J **24:** 1664–1673

Varnai P, Balla T (1998) Visualization of phosphoinositides that bind pleckstrin homology domains: calcium- and agonist-induced dynamic changes and relationship to myo-[^{3}H]inositol-labeled phosphoinositide pools. J Cell Biol **143:** 501–510

Veri MC, DeBell KE, Seminario MC, DiBaldassarre A, Reischl I, Rawat R, Graham L, Noviello C, Rellahan BL, Miscia S, et al (2001) Membrane raft-dependent regulation of phospholipase Cgamma-1 activation in T lymphocytes. Mol Cell Biol **21:** 6939–6950

Waugh MG, Lawson D, Tan SK, Hsuan JJ (1998) Phosphatidylinositol 4-phosphate synthesis in immunoisolated caveolae-like vesicles and low buoyant density non-caveolar membranes. J Biol Chem **273:** 17115–17121

Wissing JB, Kornak B, Funke A, Riedel B (1994) Phosphatidate kinase, a novel enzyme in phospholipid metabolism (characterization of the enzyme from suspension-cultured *Catharanthus roseus* cells). Plant Physiol **105:** 903–909

Xu L, Shen Y, Joseph T, Bryant A, Luo JQ, Frankel P, Rotunda T, Foster DA (2000) Mitogenic phospholipase D activity is restricted to caveolin-enriched membrane microdomains. Biochem Biophys Res Commun **273:** 77–83

Zalejski C, Paradis S, Maldiney R, Habricot Y, Miginiac E, Rona JP, Jeannette E (2006) Induction of abscisic acid-regulated gene expression by diacylglycerol pyrophosphate involves Ca^{2+} and anion currents in Arabidopsis suspension cells. Plant Physiol **141:** 1555–1562

Zalejski C, Zhang Z, Quettier AL, Maldiney R, Bonnet M, Brault M, Demandre C, Miginiac E, Rona JP, Sotta B, et al (2005) Diacylglycerol pyrophosphate is a second messenger of abscisic acid signaling in Arabidopsis thaliana suspension cells. Plant J **42:** 145–152